Out-of-Core Solver Based DDM for Solving Large Airborne Array

Yan Yan Li, Xun Wang Zhao, and Huan Huan Zhang

School of Electronic Engineering
Xidian University, Xi'an, Shaanxi 710071, China
liyanyan0418@126.com, xdzxw@126.com, zhanghuanajkd@outlook.com

Abstract ─ In this paper, we present a new methodology for an overlapping domain decomposition by using higher-order MoM and out-of-core solver (HO-OC-DDM) for analyzing large electromagnetic (EM) problems. This paper proposes two main novelties. First, the required number of meshes is decreased with the application of new higher-order basis function in the discretization of integral equation (IE). As a consequence, the number of unknowns for large EM problems can be reduced. Second, a parallel out-of-core solver is presented in this paper, which can accelerate the matrix filling and solving process without loss of accuracy. The out-of-core solver breaks the limitation of computer RAM and can be efficiently implemented in domain decomposition method (DDM).

Index Terms ─ Domain decomposition method, higher-order MoM, integral equation, out-of-core.

I. INTRODUCTION

The computer simulation has emerged as a powerful and indispensable tool in engineering design and analysis. Integral equations (IE) method, only the discretization of the surface of the object and with high accuracy, has been widely used for analyzing EM problems [1]. However, it will result in a large and dense matrix for the analysis of electrically large problems. Considering that we are interested in studying airborne antenna radiation on a large platform, such as an aircraft. The electromagnetic radiation and scattering from both the antennas and the platform need to be simulated accurately. Such an EMC problem is extremely challenging and is possibly beyond the capabilities of any conventional numerical methods. Domain decomposition method (DDM) could be an effective way to solve the EM properties from electrically large problem [2]. Combining the method of integral equations with DDM should enable some problems that we faced to be solved.

The DDM have been commonly applied in finite elements, finite difference and integral equations methods [3-6]. Among them, the domain decomposition method based on integral equations for the solution of electromagnetic radiation and scattering problems has proved its ability in solving complex EM problems, but the scale of the problem is small, which cannot satisfy the demand for solving electrically large problem, such as airborne array. In addition, the introduction of fast algorithm would further bring into error, reducing the accuracy and iterative convergence speed. Reference [7] discussed the multiple existing CEM solvers DDM, which employ diffident techniques for each of the subdomains, such as MoM and FEM. This method has been successfully used to model multiple antennas on a large air platform. However, the CPU time and storage for each subdomain are very large when simulating an even large problem or the frequency is enhanced.

A new solution scheme based on overlapping domain decomposition method, higher-order MoM and parallel out-of-core solver, called as HO-OC-DDM, is proposed in this paper. The greatest advantage of the out-of-core solver [8] is that during the evaluation of the matrix elements and its solution through the LU decomposition, the original matrix is decomposed into a set of smaller matrices fitted in-core. This technique extends the capability of MoM to solve problems, which can be as large as the amount of storage on the hard disk. For HO-OC-DDM, the simulation model is divided into several parts and out-of-core MoM is employed for each part. Moreover, higher-order basis functions are used to approximate the current distribution [8-9], which produce fewer unknowns than lower-order basis functions and further increase the scale of the problem to be solved. This method provides unprecedented flexibility and convenience for the object with changeable parts, since it just needs to re-compute the changed portion of the model during the design process, such as the analysis of antenna distribution on airborne system.

The rest of this paper is organized as follows. In Section II, the algorithm of DDM, higher-order basis function and out-of-core scheme is presented. Section III provides numerical examples to demonstrate the correctness and robustness of the proposed method.

Finally, some conclusions are given in Section IV.

II. FORMULATION

A. Domain decomposition method

The 3D EM scattering or radiation problem of an arbitrarily shaped object can be modeled with surface integral equations (SIE) [10]. The surface of the object is discretized into many quadrangle patches, and then the integral equation can be represented by a matrix equation using high order basis functions, which will be discussed in the next section. The matrix equation is as follows:

$$\mathbf{ZI} = \mathbf{V}, \qquad (1)$$

where the coefficient matrix Z is an $M \times M$ square matrix, I is the unknown current coefficient vector and V is the vector of excitation.

As shown in Fig. 1, the entire problem is divided into n subdomains Ω_i ($i=1,2\ldots n$), each subdomain is extended with its buffer regions as $\tilde{\Omega}_i = \Omega_i + \Omega_{\mathrm{F}i} + \Omega_{\mathrm{B}i}$, the dot line in Fig. 1, $\Omega_{\mathrm{F}i}$ and $\Omega_{\mathrm{B}i}$ are the forward and backward buffer regions. Ω_i denotes as the ith subdomain. The matrix Equation (1) can be expressed as:

$$\begin{bmatrix} \mathbf{Z}_{11} & \mathbf{Z}_{12} & \cdots & \mathbf{Z}_{1n} \\ \mathbf{Z}_{21} & \mathbf{Z}_{22} & \cdots & \mathbf{Z}_{2n} \\ \vdots & \vdots & & \vdots \\ \mathbf{Z}_{n1} & \mathbf{Z}_{n2} & \cdots & \mathbf{Z}_{nn} \end{bmatrix} \begin{bmatrix} \mathbf{I}_1 \\ \mathbf{I}_2 \\ \vdots \\ \mathbf{I}_n \end{bmatrix} = \begin{bmatrix} \mathbf{V}_1 \\ \mathbf{V}_2 \\ \vdots \\ \mathbf{V}_n \end{bmatrix}, \qquad (2)$$

where $Z_{ij}\,(i=j)$ is the self-impedance matrix in Ω_i, $Z_{ij}\,(i \neq j)$ is the mutual impedance matrix between Ω_j and Ω_i, I_i is the current coefficient vector in Ω_i and V_i is the excitation vector in Ω_i.
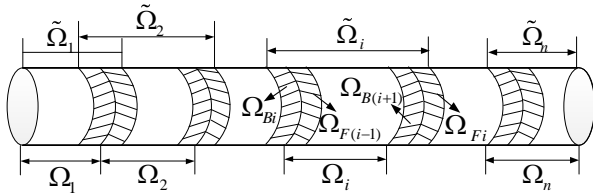

Fig. 1. Notations for domain decomposition.

The excitation in the computational subdomain includes both the information of incident plane wave and the coupling from the other subdomains, which can be calculated using the newly restricted currents after discarding the currents in bilateral buffer regions. Thus, the current edge effects in both sides are depressed and then the convergence is accelerated [11].

As all of the subdomains are extended with the buffer regions, the Gauss-Seidel iterative procedure should be modified here. Initialize the number of iteration $k=0$, the currents in all subdomains $I_i^{(0)}=0$ ($i=1, 2,\ldots,n$) and the error limitation δ. Set $k=1, 2 \ldots$, the iterative scheme inform of matrix equation can be expressed as:

$$\tilde{\mathbf{I}}_i^{(k)} = -\tilde{\mathbf{Z}}_{ii}^{-1} \sum_{j<i} \tilde{\mathbf{Z}}_{ij} \mathbf{I}_j^{(k)} - \tilde{\mathbf{Z}}_{ii}^{-1} \sum_{j>i} \tilde{\mathbf{Z}}_{ij} \mathbf{I}_j^{(k-1)} + \tilde{\mathbf{Z}}_{ii}^{-1} \tilde{\mathbf{V}}_i, \qquad (3)$$

where $\tilde{\mathbf{Z}}_{ii}$ is the self-impedance matrix in $\tilde{\Omega}_i$, $\tilde{\mathbf{Z}}_{ij}$ is the mutual impedance matrix between Ω_j (discard the overlap region) and $\tilde{\Omega}_i$, $\tilde{\mathbf{I}}_i^{(k)}$ is the vector of current coefficients in $\tilde{\Omega}_i$ to be solved during the kth iteration, $\mathbf{I}_j^{(k)}$ is the vector of current coefficients in Ω_j (discard the overlap region) at the kth iteration, $\tilde{\mathbf{V}}_i$ is the excitation vector in $\tilde{\Omega}_i$.

The relative residual error at kth iteration is used for expressing the convergence behaviour of the iterative method, which is defined as:

$$error(k) = \max\left\{\left\|\mathbf{I}_i^{(k)} - \mathbf{I}_i^{(k-1)}\right\| / \left\|\mathbf{I}_i^{(k)}\right\|\right\} \quad (i=1,2,\ldots,n). \quad (4)$$

The iteration will not stop until the error $(k) \leq \delta$.

Noting that the mutual impedance in Equation (3) is actually unnecessary to be stored during the procedure, the coupling voltage can be obtained using the near field produced by the current. The inverse of self-impendence for each subdomain is computed using the parallel and out-of-core LU decomposition algorithm and will be reused. In this way, the computing procedure can be largely accelerated.

B. High-order MoM and out-of-core solver

The object under consideration is firstly decomposed into several subdomains. Because antennas usually contain metallic and dielectric materials, the integral equation employed is the PMCHW formulation [10]. Both electric and magnetic currents are used for electromagnetic modeling of dielectric components. The geometric modeling is achieved by using bilinear quadrilateral patches to characterize, as shown in Fig. 2. Efficient approximation for the unknown currents is obtained by using higher-order basis functions (5):

$$\mathbf{F}_{ij}(p,s) = \frac{\boldsymbol{\alpha}_s}{\left|\boldsymbol{\alpha}_p \times \boldsymbol{\alpha}_s\right|} p^i s^j, -1 \leq p \leq 1, -1 \leq s \leq 1, \quad (5)$$

where p and s are the local coordinates, i and j are the orders of basis functions, and $\boldsymbol{\alpha}_p$ and $\boldsymbol{\alpha}_s$ are covariant unitary vectors. The polynomials can also be used as the basis functions for wire structures. In this case, truncated cones are used for geometric modeling [9].

The capacity of the RAM available for our high performance cluster is 8700 GB, which can support a double-precision complex matrix of order at most 764098, which is too small for electrically large problems. However, it is noticed that the total hard disk storages available are about 200TB. If the disk storage can be used instead of RAM, the scale of problem that can be solved will largely increase. The main feature of out-of-core algorithm is the original full matrix is decomposed into a set of smaller matrices that can be

fitted in-core. The (double-precision complex) matrix with M rows and columns requires $N_{\text{storage}} = M \times M \times 16$ bytes of hard-disk storage. The computer system has M_{RAM} bytes of in-core buffer available to each process. To complete the decomposition of the matrix, each process will handle a specific number of portions I_{slab}:

$$I_{\text{slab}} = ceiling \left\{ \frac{N_{\text{storage}}}{p M_{\text{RAM}}} \right\}, \qquad (6)$$

where p is the total number of processes, and the *ceiling* function returns the smallest integer greater than or equal to the number.

milestone

Fig. 2. Bilinear quadrilateral patch defined by four vertices with r_{11}, r_{12}, r_{21} and r_{22}.

Setting the decomposition is oriented along the column, as shown in Fig. 3, one slab consisting of M rows of the matrix by the number of columns that will fit in the total amount of the in-core buffer available.

The width of ith out-of-core slab is K_i, thus:

$$M = \sum_{i=1}^{I_{\text{slab}}} K_i. \qquad (7)$$

The width of last slab ($i=I_{\text{slab}}$) K_{last} is:

$$K_{last} = M - \sum_{i=1}^{I_{\text{slab}}-1} K_i. \qquad (8)$$
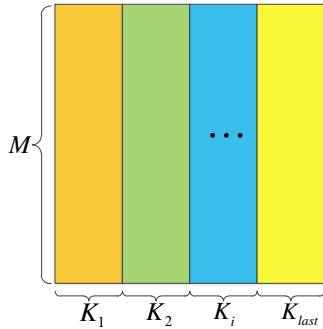

Fig. 3. Data decomposition for storing an out-of-core matrix.

The assignment to fill each slab is distributed over p processes by using the block distribution scheme of ScaLAPACK or PLAPACK [8]. It is important that the matrix filling schemes should be designed to avoid redundant calculation for better parallel efficiency. For the out-of-core LU factorization, the one-slab left-looking out-of-core algorithm is applied and the right-looking in-core algorithm is used when factoring each slab. Thus, the advantages of both the left-looking and the right-looking algorithms are retained. The detail of parallel out-of-core algorithm for MoM can be found in [9].
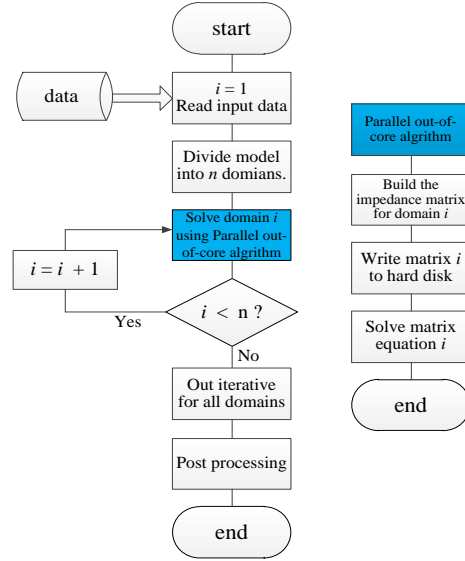
The flowchart of the HO-OC-DDM is shown in Fig. 4.

Fig. 4. Flowchart of HO-OC-DDM.

III. NUMERICAL RESULTS

Three EM examples are presented to demonstrate the efficiency and accuracy of the proposed method. The residual error for outer iterative convergence is set to 3.0e–3 without any specification. Two computational platforms are used in this paper.

Platform I: A workstation with two six-core 64 bit Intel Xeon E5-2620 2.0 GHz CPUs, 64 GB RAM and 6TB disk.

Platform II: High-Performance Computing (HPC) cluster with 136 computing nodes. Each computing node has two 12-core bit Intel Xeon E5-2692 2.2 GHz CPUs, 64 GB RAM and 1.8TB disk.

A. An umbrella microstrip array with 30×1 elements

To validate the accuracy and efficiency of the proposed HO-OC-DDM for discontinuous problems, an umbrella microstrip array with 30×1 elements of umbrella microstrip patch is simulated. As shown in Fig. 5, the dielectric substrate of the antenna is 0.8 mm in thickness and ε_r=10.2. The array is divided into two equal sized sub-domains and the overlap part is unnecessary for the subdomains are discontinuous in geometry.

The simulation is performed on Platform I, and the operating frequency is 2.5 GHz. The two-dimensional

(2D) radiation patterns obtained by the proposed HO-OC-DDM are shown in Fig. 6. The patterns of overall solution using high-order MoM and the MoM from FEKO software are also given for comparison. The number of unknowns of the microstrip array is 24330 for higher-order MoM and 60115 for MoM (FEKO). To compare out-of-core performance of the proposed method with MoM (FEKO) in the same number of unknowns, an umbrella microstrip array with 25×3 elements is simulated using MoM (HO-OC). It can be seen that the results agree with each other very well. For the HO-OC-DDM, the computer memory is reduced by a half (see Table 1), the CPU time is not sharply reduced when simulating a small problem. For the overall solution of microstrip array with 30×1 elements, MoM (HO-OC) costs 625s and MoM (FEKO) costs 16571s. For the microstrip array with 25×3 elements, which has the same number of unknowns with MoM (FEKO), the CPU time of MoM (HO-OC) is 11554s.
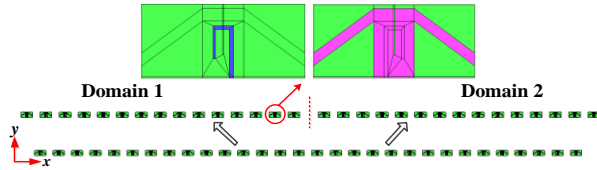

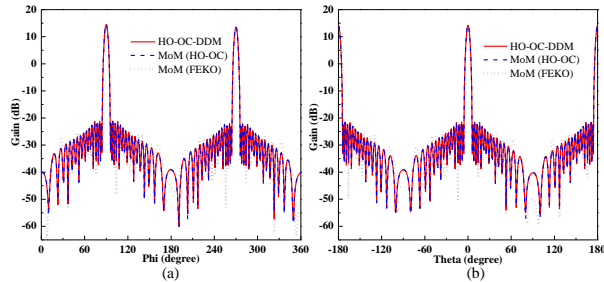Fig. 5. Model of umbrella microstrip array with 30×1 elements.

Fig. 6. 2D radiation patterns of the umbrella microstrip array: (a) x-y and (b) x-z.

Table 1: Computational statistics of umbrella microstrip array

Method	Unknowns	Storage (GB)	CPU Time(s)
DDM	12165(domain 1)	4.41	720
	12165(domain 2)		
MoM (HO-OC)	24330(30×1)	8.82	967
	60825(25×3)	55.13	11554
MoM (FEKO)	60115(30×1)	53.85	16571

B. A rectangle microstrip array with 20×4 elements

Consider a rectangle patch microstrip array with 20×4 elements as shown in Fig. 7. The units are connected with each other. The thickness of dielectric substrate is 0.018 m and ε_r=4.5, the operating frequency is 440 MHz, the dimension of antenna is 5.27 m × 0.95 m. The model is divided into two overlapping subdomains (extending two units into each other) in this example.

The simulation is performed on Platform I. The radiation patterns of the antenna array obtained by HO-OC-DDM and the overall solution by higher-order MoM are shown in Fig. 8. They are in good agreement with each other. The computational statistics for solving each subdomain and entire problem are recorded in Table 2. It can be observed that the HO-OC-DDM leads to over 25% memory reduction compared with the overall solution for this example.
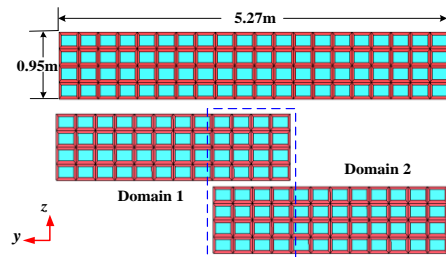

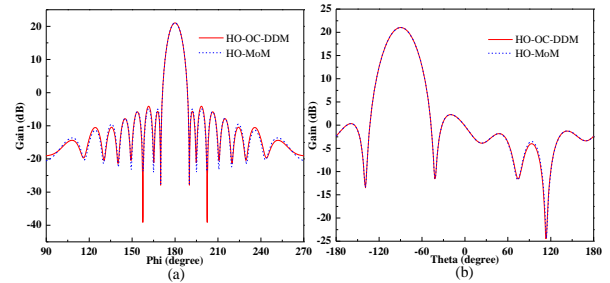Fig. 7. Model of rectangle microstrip array with 20×4 elements.

Fig. 8. 2D radiation patterns of the rectangle microstrip array: (a) x-y and (b) x-z.

Table 2: Computational statistics of rectangle microstrip array

Method	Unknowns	Storage (GB)	CPU Time(s)
DDM	12000(domain 1)	4.28	951
	12000(domain2)		
MoM	19840	5.86	1080

C. Radiation of a dipole array above a PEC cylinder

The radiation of a dipole array above a PEC cylinder is simulated in this example to discuss the effect of the size of buffer region. As shown in Fig. 9, the radius and length of cylinder is 1.5 m and 18 m. The working frequency is 1.0 GHz. The dipole antenna is located

above the cylinder and the direction of feeder is +x. As shown in Fig. 9, the model is divided into four subdomains. The antenna represents domain 1, and each color of the cylinder represents the rest three subdomains. Three different sizes of buffer region, 0.5λ, 1λ and 1.5λ, is considered during the simulation.

The simulation is performed on Platform I. The 2D radiation pattern of the object obtained by HO-OC-DDM is shown in Fig. 10 and the overall solution by MoM is also given for comparing. Compared with 0.5λ buffer region, the results of 1λ and 1.5λ buffer region are in good agreement with that of the overall solution. The computational statistics for solving each subdomain are accorded in Table 3. As shown in Fig. 10, the accuracy is good enough in engineer application when the size of the buffer region increase to 1λ.

The memory and CPU time are increasing while the size of buffer region is enlarging. The root mean square error (RMSE) of radiation for different size of buffer region is defined as $RMSE = \sqrt{\dfrac{\left\| Gain^{DDM} - Gain^{MoM} \right\|_2^2}{n}}$, where $Gain^{DDM}$ is the gain vector obtained by the proposed method and $Gain^{MoM}$ is the overall solution vector obtained by high-order MoM. When size of buffer regions are 0.5λ, 1λ and 1.5λ, the RMSE of the proposed method is 0.1193, 0.0871 and 0.0892 respectively. Considering the simulation accuracy and computation resources, the buffer region with 1λ size is acceptable in this method.
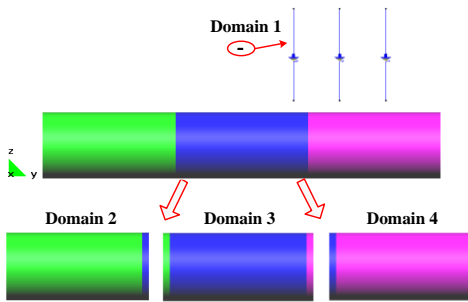
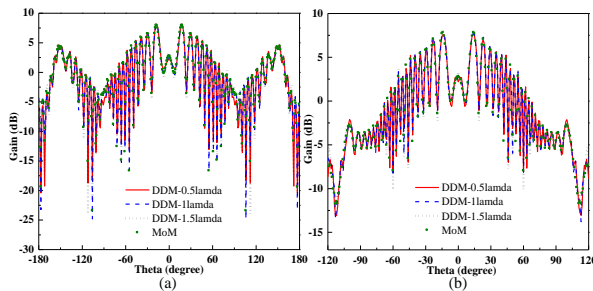

Fig. 9. Model of a dipole array above a PEC cylinder.

Fig. 10. 2D radiation patterns of the dipole antenna above a cylinder: (a) x-z and (b) y-z.

Table 3: Computational statistics of rectangle microstrip array

Method	Buffer Region	Unknowns	Storage (GB)	CPU Time(s)
DDM	0.5λ	9	16.41	1680
		18704		
		19824		
		18928		
	1λ	9	17.73	1750
		19152		
		20944		
		19600		
	1.5λ	9	19.67	2100
		20048		
		22512		
		20272		
MoM	19840	53657	42.9	5674

D. Radiation of phased airborne array with 55×15 elements

The accuracy of the proposed method has been proved in the above two examples. An electrically large problem for engineering application will be solved in this example. Consider a 55×15 microstrip patch array mounted on an airplane, as illustrated in Fig. 11. The antenna array is arranged on x-z plane. The dimensions of patch are 0.144 m × 0.072 m × 0.00072 m, and the distance between two neighboring elements is 0.1225 m along both the length and width directions. The working frequency of the array is 2.0 GHz. The array is installed 5.0 m above an airplane that is 36 m long, 40.0 m wide and 10.5 m high, and the distance between the center of the array and the nose of the airplane is 17.8 m.

A −40 dB Taylor distribution is utilized in the array feed along the x-direction and −25 dB along the z-direction, the mainlobe is directed towards the tail and sweeps 5° and 10° toward the wing. The number of unknowns of the airborne array is 1,569,836, which is too large for the computing resource available. However, the problem can be solved by the HO-OC-DDM. In this example, we divide the model into eight sub-domains as shown in Fig. 12. Each color represents a subdomain respectively. The simulation is performed on Platform II and 720 CPU cores are used.
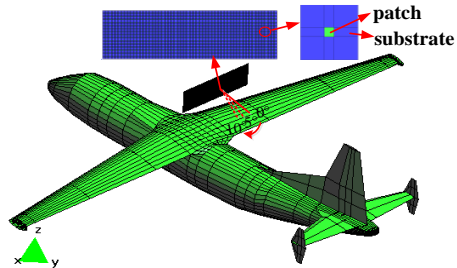

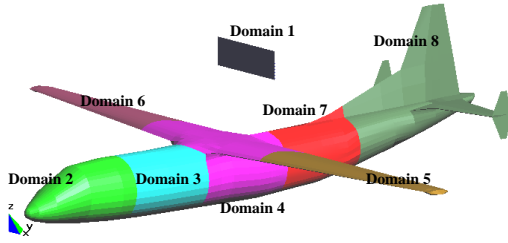Fig. 11. Model of airborne antenna array.

Fig. 12. Domain decomposition model (each color represents a sub-domain).

The phased shift patterns of antenna array before and after it is mounted on the airplane are computed by the proposed HO-OC-DDM as shown in Fig. 13 and Fig. 14. The sidelobe level of the airborne array increases in the azimuth plane. Furthermore, there is a decrease in the maximum gain compared with that of the array, as shown in Fig. 13. The deterioration of the patterns is most serious when the mainlobe is directed towards the tail. In Table 4, a comparison of the computational statistics between the HO-OC-DDM and MoM is shown. It is worth noting that the overall CPU time include two parts, subdomains solution time and iteration time. In the solution time, the computing time for platform is 3.52h and the iteration time is only 0.66h. For the phased airborne array, the platform subdomains (domain 2-8) are unchanged and can be reused during the solution. Thus, the memory requirement and CPU time are greatly reduced. The proposed method is of great significance especially for the solution of very large problems in engineering application
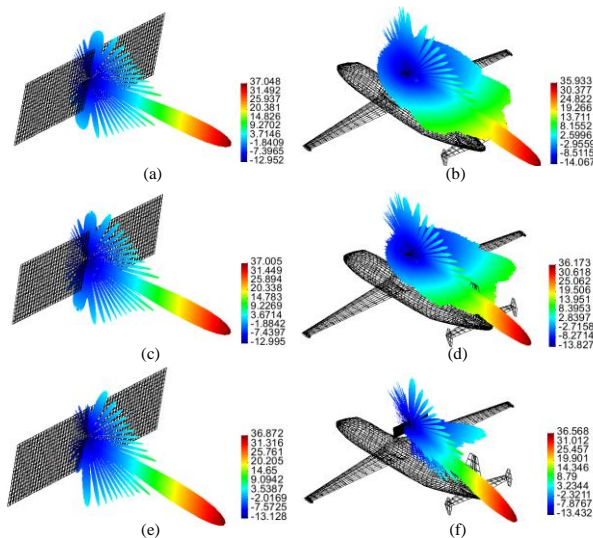

Fig. 13. 3D radiation patterns of phased airborne array: (a) the array with scan 0°, (b) the array over the airplane with scan 0°, (c) the array with scan 5°, (d) the array over the airplane with scan 5°, (e) the array with scan 10°, and (f) yhe array over the airplane with scan 10°.
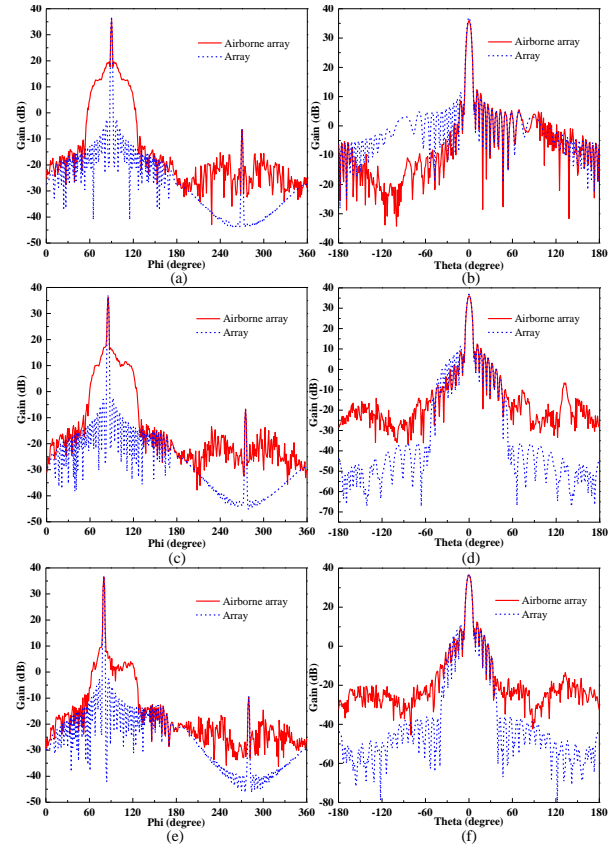

Fig. 14. 2D radiation patterns of phased airborne array: (a) azimuth plane pattern with scan 0°, (b) elevation plane pattern with scan 0°, (c) azimuth plane pattern with scan 5°, (d) elevation plane pattern with scan 5°, (e) azimuth plane pattern with scan 10°, and (f) elevation plane pattern with scan 10°.

Table 4: Computational statistics of airborne array

Method	Unknowns	Storage (TB)	CPU Time (h)
DDM	305408(1)	1.36	3.05 (1)
	96524(2)	0.14	
	95073(3)	0.13	
	212711(4)	0.66	3.52 (2-8)
	102207(5)	0.16	
	102753(6)	0.16	
	97261(7)	0.14	
	247282(8)	0.89	17.23 (total)
MoM	1569836	35.86	— —

IV. CONCLUSION

An efficient HO-OC-DDM algorithm is developed to solve large complex problem such as airborne array. Particularly, our emphasis herein is the combination of out-of-core technology, higher order MoM and domain decomposition method, which allows the matrices for each domain to be written in the hard disk, extending the capacity of MoM based domain decomposition methods.

Moreover, the proposed method is also suitable for solving the problems with changeable parts.

REFERENCES

[1]   R. F. Harrington, *Field Computations by Moment Methods*. Macmillan, New York, 1968.

[2]   L. Yin, J. Wang, and W. Hong, "A novel algorithm based on the domain-decomposition method for the full-wave analysis of 3D electromagnetic problems," *IEEE Trans. Microw. Theory Tech.*, vol. 50, no. 8, pp. 2011-2017, 2002.

[3]   Z. Lou and J. M. Jin, "A novel dual-field time-domain finite-element domain-decomposition method for computational electromagnetics," *IEEE Trans. Antennas Propagat.*, vol. 54, no. 6, pp. 1850-1862, 2006.

[4]   Z. H. Lai, J. F. Kiang, and R. Mittra, "A domain decomposition finite difference time domain (FDTD) method for scattering problem from very large rough surfaces," *IEEE Trans. Antennas Propagat.*, vol. 63, no. 10, pp. 4468-4476, 2015.

[5]   W. D. Li, W. Hong, and H. X. Zhou, "Integral equation-based overlapped domain decomposition method for the analysis of electromagnetic scattering of 3D conducting objects," *Microwave and Optical Technology Letters*, vol. 49, no. 2, pp. 265-274, 2007.

[6]   S. M. Rao, "A true domain decomposition procedure based on method of moments to handle electrically large bodies," *IEEE Trans. Antennas Propagat*., vol. 60, no. 9, pp. 4233-4238, 2012.

[7]   X. C. Wang, Z. Peng, and J. F. Lee, "Multisolver domain decomposition method for modeling EMC effects of multiple antennas on a large air platform," *IEEE Trans. Electromagn. Compat*., vol. 54, no. 2, pp. 375-388, 2012.

[8]   Y. Zhang, R. A. van ce Geijn, M. C. Taylor, and T. K. Sarkar, "Parallel MoM using higher order basis function and PLAPACK in-core and out-of-core solvers for challenging EM simulations," *IEEE Antennas Propagat. Magazine*, vol. 51, no. 5, pp. 42-60, 2009.

[9]   Y. Zhang and T. K. Sarkar, *Parallel Solution of Integral Equation Based EM Problems in the Frequency Domain. Hoboken*, Hoboken NJ, USA: Wiley, 2009.

[10] G. Mumcu, K. Sertel, and J. Volakis, "Surface integral equation solution for modeling 3-D uniaxial media using closed-Form dyadic Green's functions," *IEEE Trans. Antennas Propagat.*, vol. 56, no.8, pp. 2381-2388, 2008.

[11] W. D. Li, W. Hong, and H. X. Zhou, "An IE-ODDM-MLFMA scheme with DILU preconditioner for analysis of electromagnetic scattering from large complex objects," *IEEE Trans. Antennas Propagat.*, vol. 56, no. 5, pp. 1368-1380, 2008.

Li Yanyan received the B.S. degree from Xinzhou Teacher's University, Shanxi, China, in 2012, and is currently working toward the Ph.D. degree at Xidian University. Her current research interests is computational electromagnetic.

Xunwang Zhao received the B.S., and Ph.D. degrees from Xidian University, Xi'an, China, in 2004, and 2008, respectively. He joined Xidian University as a Faculty Member in 2008. As Principal Investigator, he is doing or has completed some projects including project of NSFC.

Huan Huan Zhang received the Bachelor degree in Electronic Information Engineering from Henan Polytechnic University in 2009, the Ph.D. degree in Electromagnetic Fields and Microwave Technology from Nanjing University of Science and Technology in 2015. He was a Post-doctoral Fellow with the Center of Electromagnetics and Optics, the University of Hong Kong, Hong Kong, from 2015 to 2016. He is currently a Lecturer with the School of Electronic Engineering, Xidian University, Xi'an, China.

Zhang serves as the Reviewer of the IEEE Transactions on Antenna and Propagation, Communications in Computational Physics, IET Radar, Sonar & Navigation, etc. His current research interests include computational electromagnetics, IC signal and power integrity, EMC/EMI and radar signal processing.